

# Estimating the influence of finite instrumental resolution on elastic neutron scattering intensities from proteins

Gerald R. Kneller<sup>a)</sup>

*Centre de Biophysique Moléculaire, CNRS,<sup>b)</sup> Rue Charles Sadron, 45071 Orleans, France  
and Synchrotron Soleil, L'Orme de Merisiers, BP 48, 91192 Gif-sur-Yvette, France*

Vania Calandrini

*Institut Laue-Langevin, BP 156, 38042 Grenoble, France*

(Received 2 January 2007; accepted 30 January 2007; published online 30 March 2007)

Recent experimental and simulation studies show that the fractional Ornstein-Uhlenbeck process describes well the single particle motions in internal protein dynamics. Here the authors use this model to estimate the influence of finite instrumental resolution on elastic neutron scattering intensities from hydrated protein powders. They give, in particular, an estimation of the attenuation factor for the observed atomic position fluctuations, assuming a Gaussian and a triangular resolution function. © 2007 American Institute of Physics. [DOI: [10.1063/1.2711207](https://doi.org/10.1063/1.2711207)]

## I. INTRODUCTION

A large part of the investigation of protein dynamics by neutron scattering techniques has been devoted to studying the so-called “glass transition,” which occurs in many proteins at about 200 K.<sup>1–3</sup> Below that temperature one observes essentially harmonic vibrations about a local minimum of the potential energy and above 200 K an onset of diffusive motions. On the time scale of neutron scattering experiments, which is situated in the picosecond to nanosecond range, the diffusive motions are dominated by “liquidlike” rigid-body motions of the protein side chains.<sup>4</sup> One must, however, be aware that relaxation processes in proteins cover an enormous spectrum of relaxation times, ranging from picoseconds to hours. This has been evidenced by recent studies of the functional dynamics of proteins based on fluorescence correlation spectroscopy<sup>5</sup> (FCS) and by studying the kinetics of ligand rebinding upon flash photolysis.<sup>6</sup> These techniques are sensitive to protein relaxation dynamics in the time range of milliseconds to hours. Such slow stochastic processes are characterized by a strongly nonexponential decay of the time correlation functions under consideration, indicating a broad distribution of relaxation rates. To account for this fact, the kinetic studies mentioned above have been phenomenologically described by a time correlation function which is the solution of a fractional differential equation.<sup>7</sup> A slightly more physical model has been used to interpret the FCS experiments, assuming that the distance between different parts of a protein, here a fluorophore and a quencher, can be described by fractional Brownian dynamics (fBD) in a harmonic potential.<sup>5,8</sup> The model is a generalization of the well known Ornstein-Uhlenbeck process<sup>9</sup> and accounts for the spatial confinement of internal protein motions as well as for a broad spectrum of relaxation rates. A characteristic feature of the model is the absence of a typical time scale and a corre-

sponding fractal behavior of the time correlation functions and their Fourier spectra. Recent investigations have, in particular, shown that fBD in a harmonic potential captures also well the relaxation dynamics of proteins on the much shorter pico- to nanosecond time scale and may thus be used to interpret quasielastic and elastic neutron scattering (QENS/ENS) experiments.<sup>10,11</sup> Static correlation functions are the same as for the simple harmonic oscillator model, which has been used to relate the average position fluctuation to an effective force constant characterizing the “resilience” of a protein.<sup>12</sup> Essential mechanical properties and multiscale relaxation are thus covered by the same theoretical description, and contact can also be made with the more realistic multi-component Gaussian model of coupled overdamped Langevin oscillators.<sup>13</sup> We note here that the model of a particle diffusing in a spherical cavity<sup>14</sup> has been frequently used in the past in order to describe QENS studies of intramolecular protein dynamics. This description accounts for spatial confinement of atomic motions inside a protein, but not for multiscale relaxation processes, which are characteristic for protein dynamics.

The purpose of this article is to use fBD in a harmonic potential as a model for correcting elastic neutron scattering experiments for unwanted quasielastic contributions due to finite instrumental resolution. Although such experiments do not aim at exploring the atomic dynamics in proteins, they are biased by slow relaxation processes which are too slow to be detected by the neutron spectrometer and are counted as “elastic.” Recently this problem has regained interest and has been tackled by different research groups.<sup>15,16</sup> Here we use an analytical approach which relies on the capability of the fBD model to extrapolate the slow relaxation dynamics *a priori* to arbitrarily long time scales. The article is organized as follows: In Sec. II we present the fractional Ornstein-Uhlenbeck process as a model for internal protein dynamics and its implications for the resulting correlation functions measured in QENS and ENS experiments. Section III is then devoted to the application of the model to correct measured

<sup>a)</sup> Author to whom correspondence should be addressed. Electronic mail: [kneller@cns-orleans.fr](mailto:kneller@cns-orleans.fr)

<sup>b)</sup> Affiliated with the University of Orléans.

elastic intensities for unwanted quasielastic contributions and the article is concluded by a short résumé of the results.

## II. FRACTIONAL ORNSTEIN-UHLENBECK PROCESS

### A. Fokker-Planck equation

In the following we consider a particle whose dynamics can be modeled by fBD in a harmonic potential of the form ( $K > 0$ )

$$V(x) = \frac{1}{2}Kx^2. \quad (2.1)$$

For our purposes it is sufficient to consider a one-dimensional problem of a particle diffusing along the  $x$  coordinate in a Cartesian coordinate system. From a probabilistic point of view, fBD in a harmonic potential is described by a phenomenological, non-Markovian extension of the Fokker-Planck equation for the Ornstein-Uhlenbeck (OU) process<sup>17</sup>

$$\frac{\partial P(x,t)}{\partial t} = \tilde{\tau}^{1-\alpha} {}_0\mathcal{D}_t^{1-\alpha} \mathcal{L}_{\text{FP}} P(x,t). \quad (2.2)$$

Here  $P(x,t) \equiv P(x,t|x_0,t_0)$  denotes the transition probability density for a move from position  $x_0$  at time  $t_0$  to position  $x$  at time  $t$ , and  $\mathcal{L}_{\text{FP}}$  is the Fokker-Planck operator<sup>18,19</sup>

$$\mathcal{L}_{\text{FP}} = \eta \frac{\partial}{\partial x} x + D \frac{\partial^2}{\partial x^2}. \quad (2.3)$$

The two positive constants  $\eta$  and  $D$  are, respectively, the relaxation rate and the short-time diffusion constant of the OU process, which are related by the mean square position fluctuation of the diffusing particle,

$$\langle x^2 \rangle = \frac{D}{\eta} = \frac{k_B T}{K}. \quad (2.4)$$

As usual,  $k_B$  denotes the Boltzmann constant and  $T$  the absolute temperature in Kelvin. The operator  ${}_0\mathcal{D}_t^{1-\alpha}$  stands for a fractional derivative of order  $1-\alpha$ .<sup>7</sup> Its action on an arbitrary function  $f(\cdot)$  is defined through

$${}_0\mathcal{D}_t^{1-\alpha} f(t) = \frac{d}{dt} \int_0^t d\tau \frac{(t-\tau)^{\alpha-1}}{\Gamma(\alpha)} f(\tau), \quad (2.5)$$

where  $\Gamma(\cdot)$  is the Gamma function.<sup>20</sup> The time scale parameter  $\tilde{\tau}$  is introduced to ensure the correct physical dimension of the right-hand side of Eq. (2.2).

The solution of the fractional Fokker-Planck equation [Eq. (2.2)] has been described in the literature,<sup>8,10,17</sup> and we give directly the result

$$P(x',t|x'_0,0) = \frac{\exp(-x'^2/2)}{\sqrt{2\pi}} \sum_{n=0}^{\infty} \frac{1}{2^n n!} H_n\left(\frac{x'}{\sqrt{2}}\right) H_n\left(\frac{x'_0}{\sqrt{2}}\right) \times E_\alpha(-n\eta_\alpha t^\alpha). \quad (2.6)$$

Here  $H_n(\cdot)$  are the Hermite polynomials<sup>20</sup> and  $x'$  are the scaled positions

$$x' = \frac{x}{\sqrt{\langle x^2 \rangle}}. \quad (2.7)$$

The symbol  $E_\alpha(\cdot)$  denotes the Mittag-Leffler function,<sup>21</sup> which has the series representation ( $z \in \mathbb{C}$ )

$$E_\alpha(z) = \sum_{k=0}^{\infty} \frac{z^k}{\Gamma(1+\alpha k)}, \quad (2.8)$$

and  $\eta_\alpha$  is the scaled, “fractional” relaxation constant

$$\eta_\alpha = \tilde{\tau}^{1-\alpha} \eta. \quad (2.9)$$

One observes that the normal exponential function is retrieved from the Mittag-Leffler function by setting  $\alpha=1$ .

### B. Position autocorrelation function

It is illustrative to consider the position correlation function associated with the stochastic model described above,

$$c_{xx}(t) = \int \int dx dx_0 P(x,t;x_0,0) x x_0. \quad (2.10)$$

Assuming a stationary process, the joint probability density takes the form  $P(x,t;x_0,0) = P(x,t|x_0,0) P_{\text{eq}}(x_0)$ , where  $P(x,t|x_0,0)$  is the solution of the fractional Fokker-Planck equation [Eq. (2.2)], which is given by expression (2.6), and  $P_{\text{eq}}(\cdot)$  is the equilibrium density probability, which is defined as  $P_{\text{eq}}(x) = \lim_{t \rightarrow \infty} P(x,t|x_0,0)$ . From Eq. (2.6) one obtains

$$P_{\text{eq}}(x) = \sqrt{\frac{\eta}{2\pi D}} \exp\left(-\frac{\eta x^2}{2D}\right), \quad (2.11)$$

and the resulting position correlation function is found to be

$$c_{xx}(t) = \langle x^2 \rangle E_\alpha(-\eta_\alpha t^\alpha) \quad (t \geq 0). \quad (2.12)$$

In the following we assume that  $c_{xx}(\cdot)$  is a classical time correlation function and thus even in time,  $c_{xx}(-t) = c_{xx}(t)$ . Introducing the time scale

$$\tau = \eta_\alpha^{-1/\alpha} \quad (2.13)$$

the normalized position autocorrelation function,

$$\psi(t) := c_{xx}(t)/\langle x^2 \rangle = c_{x'x'}(t), \quad (2.14)$$

which will be considered in the following, takes the form

$$\psi(t) = E_\alpha(-[|t|/\tau]^\alpha). \quad (2.15)$$

Many interesting features of  $\psi(t)$  follow from its Laplace transform, which is defined through  $\hat{\psi}(s) = \int_0^\infty dt \exp(-st) \psi(t)$  ( $\Re\{s\} > 0$ ). From the series expansion [Eq. (2.8)] of the Mittag-Leffler function one derives

$$\hat{\psi}(s) = \frac{1}{s(1+[s\tau]^{-\alpha})}. \quad (2.16)$$

Since  $\psi(\cdot)$  is even in time, its Fourier transform,  $\tilde{\psi}(\omega) = \int_{-\infty}^{+\infty} dt \exp(-i\omega t) \psi(t)$ , can be related to its Laplace transform via  $\tilde{\psi}(\omega) = 2\Re\{\hat{\psi}(i\omega)\}$ . From Eq. (2.16) we obtain

$$\tilde{\psi}(\omega) = L_{\sigma,\tau}(\omega), \quad (2.17)$$

where  $L_{\sigma,\tau}(\omega)$  is the generalized Lorentzian<sup>11</sup>

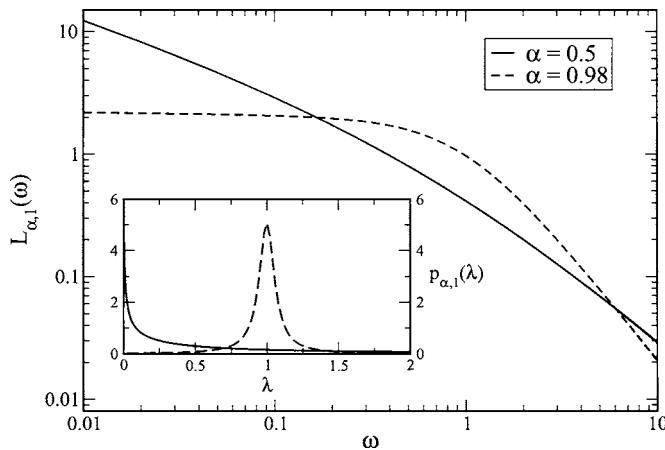


FIG. 1. Generalized Lorentzian  $L_{\alpha,1}(\omega)$  for  $\alpha=0.5$  (solid line) and  $\alpha=0.98$  (broken line). The inset shows the corresponding relaxation rate spectrum,  $p_{\alpha,1}(\lambda)$ .

$$L_{\alpha,\tau}(\omega) = \frac{2\tau \sin(\alpha\pi/2)}{|\omega\tau|(|\omega\tau|^\alpha + 2 \cos(\alpha\pi/2) + |\omega\tau|^{-\alpha})}, \quad 0 < \alpha \leq 1. \quad (2.18)$$

The nonexponential character of  $\psi(t)$  is reflected in its long time behavior, which can be derived from its Laplace transform [Eq. (2.16)] for values of  $s$  close to zero. Here  $\hat{\psi}(s) \approx \tau(s\tau)^{\alpha-1}$ , yielding

$$\psi(t) \approx \frac{(t/\tau)^{-\alpha}}{\Gamma(1-\alpha)} \quad \text{for } t \gg \tau. \quad (2.19)$$

A more detailed description of the nonexponential decay of  $\psi(t)$  is contained in the relaxation rate spectrum,  $p_{\alpha,\tau}(\lambda)$ , which is defined through the relation

$$\psi(t) = \int_0^\infty d\lambda p_{\alpha,\tau}(\lambda) \exp(-\lambda|t|). \quad (2.20)$$

It follows from  $\psi(0)=1$  that  $p_{\alpha,\tau}(\lambda)$  is normalized,  $\int_0^\infty d\lambda p_{\alpha,\tau}(\lambda) = 1$ , and the Laplace transform of  $\psi(t)$  is related to  $p_{\alpha,\tau}(\lambda)$  through a Stieltjes transform

$$\hat{\psi}(s) = \int_0^\infty d\lambda \frac{p_{\alpha,\tau}(\lambda)}{s + \lambda}. \quad (2.21)$$

The inversion of the latter is given by<sup>22</sup>

$$p_{\alpha,\tau}(\lambda) = \lim_{\epsilon \rightarrow 0^+} \frac{1}{\pi} \Im \{ \hat{\psi}(-[\lambda + i\epsilon]) \} \quad (2.22)$$

and leads to<sup>6,10</sup>

$$p_{\alpha,\tau}(\lambda) = \frac{\tau}{\pi} \frac{(\tau\lambda)^{\alpha-1} \sin(\pi\alpha)}{(\tau\lambda)^{2\alpha} + 2(\tau\lambda)^\alpha \cos(\pi\alpha) + 1}, \quad 0 < \alpha < 1. \quad (2.23)$$

The influence of the parameter  $\alpha$  on  $\tilde{\psi}(\omega)$  and the corresponding relaxation rate spectrum are shown in Fig. 1. The time scale parameter  $\tau$  is here set to one. One observes that  $p_{\alpha,1}(\lambda)$  is centered on  $\lambda=1$  if  $\alpha \rightarrow 1$ , where  $\psi(t)$  becomes an exponential and its Fourier spectrum tends to a normal Lorentzian. In the case of  $\alpha=0.5$  the relaxation rate spectrum

exhibits, in contrast, increasing contributions from small relaxation rates and the quasielastic scattering profile is almost featureless.

### C. Neutron scattering law

To make contact with neutron scattering experiments we assume that the internal dynamics of a protein can be described by a “representative” scattering atom, knowing that neutron scattering is dominated by incoherent scattering from the hydrogen atoms.<sup>23,24</sup> We assume that the system under consideration is a hydrated powder, such that translational and rotational diffusions of whole proteins can be neglected. Since such a system is isotropic we can effectively consider the projection of the atomic dynamics on the momentum transfer vector  $\mathbf{q}$ , whose direction is chosen to be along the  $x$  coordinate of a Cartesian coordinate system,  $\mathbf{q} = q\mathbf{e}_x$ . Here  $q$  is the modulus of  $\mathbf{q}$  and  $\mathbf{e}_x$  is the unit vector along the  $x$  coordinate. The incoherent intermediate scattering function is then given by

$$I(q,t) = \int \int dx dx_0 P(x,t;x_0,0) \exp(iq[x-x_0]), \quad (2.24)$$

where the joint probability is again written as  $P(x,t;x_0,0) = P(x,t|x_0,0)P_{\text{eq}}(x_0)$ . One finds the following expression for the (incoherent) intermediate scattering function:<sup>10</sup>

$$I(q,t) = \exp(-q^2\langle x^2 \rangle) \sum_{n=0}^{\infty} \frac{q^{2n}\langle x^2 \rangle^n}{n!} E_\alpha(-n\eta_\alpha t^\alpha). \quad (2.25)$$

Using the definition of the dynamic structure factor,

$$S(q,\omega) = \frac{1}{2\pi} \int_{-\infty}^{+\infty} dt \exp(-i\omega t) I(q,t), \quad (2.26)$$

one obtains from Eq. (2.25)

$$S(q,\omega) = \exp(-q^2\langle x^2 \rangle) \left\{ \delta(\omega) + \sum_{n=1}^{\infty} \frac{q^{2n}\langle x^2 \rangle^n}{n!} \frac{1}{2\pi} L_{\alpha,\tau_n}(\omega) \right\}, \quad (2.27)$$

where  $L_{\alpha,\tau}(\cdot)$  is the generalized Lorentzian defined in Eq. (2.18) and the time scales  $\tau_n$  are defined as

$$\tau_n = \pi n^{-1/\alpha}, \quad (2.28)$$

with  $\tau$  given by relation (2.13). We note that

$$\text{EISF}(q) = \exp(-q^2\langle x^2 \rangle) \quad (2.29)$$

is the elastic incoherent structure factor (EISF), which has a Gaussian form in this model and which is identical to the EISF corresponding to the standard Ornstein-Uhlenbeck process.

## III. ESTIMATING THE EISF AT FINITE RESOLUTION

### A. Approximation for the measured EISF

In the following  $r(\omega)$  is the resolution function of a neutron spectrometer, which is supposed to satisfy the normalization condition

$$\int_{-\infty}^{+\infty} d\omega r(\omega) = 1, \quad (3.1)$$

and the measured dynamic structure factor is given by the convolution integral

$$S_m(q, \omega) = \int_{-\infty}^{+\infty} d\omega' r(\omega - \omega') S(q, \omega'). \quad (3.2)$$

Convolution integrals of the above form will be abbreviated as  $(f * g)(\omega)$  in the following. We confine ourselves to the region of small  $q$  values, where the Gaussian approximation of  $I(q, t)$  can be assumed to be valid for any dynamical model.<sup>25</sup> In this case we have

$$S(q, \omega) \approx \exp(-q^2 \langle x^2 \rangle) \left\{ \delta(\omega) + q^2 \langle x^2 \rangle \frac{1}{2\pi} L_{\alpha, \tau}(\omega) \right\}. \quad (3.2')$$

The resolution function  $r(\omega)$  is supposed to have a characteristic width  $\Gamma$ , which we define to be the half width at half maximum (HWHM), in order to allow for comparisons between different resolution functions. The normalized measured elastic intensity is then given by

$$\text{EISF}_m(q) := \frac{\int_{-\Gamma}^{+\Gamma} d\omega S_m(q, \omega)}{\int_{-\Gamma}^{+\Gamma} d\omega r(\omega)}, \quad (3.3)$$

where  $r(\omega) = S_m(0, \omega)$ , irrespective of the dynamical model. For small  $q$  values one may use approximation (3.2') to obtain

$$\text{EISF}_m(q) \approx \exp(-q^2 \langle x^2 \rangle) (1 + \xi q^2 \langle x^2 \rangle), \quad (3.4)$$

where  $\xi$  is defined as

$$\xi = \frac{\int_{-\Gamma}^{+\Gamma} d\omega 1/2\pi (r * L_{\alpha, \tau})(\omega)}{\int_{-\Gamma}^{+\Gamma} d\omega r(\omega)}. \quad (3.5)$$

We note here that most authors define the measured elastic intensity as  $S_m(q, 0)$ ,<sup>15,16</sup> leading to a correction factor

$$\xi = \frac{1/2\pi (r * L_{\alpha, \tau})(0)}{r(0)}. \quad (3.6)$$

The above expression is, however, not well defined in the limit  $\Gamma \rightarrow 0$ , where the resolution function becomes a Dirac distribution,  $r(\omega) \rightarrow \delta(\omega)$ . It will be shown later that definition (3.6) leads nevertheless numerically stable results for  $\xi$ , which are similar to those obtained from definition (3.5), if  $\Gamma \tau$  stays well above machine precision.

The measured position fluctuation is obtained from the EISF via

$$\langle x^2 \rangle_m = - \frac{\partial}{\partial q^2} \ln(\text{EISF}_m(q)), \quad (3.7)$$

using small values of  $q$ , where the Gaussian approximation is valid. From expression (3.4) one obtains

$$\langle x^2 \rangle_m \approx \langle x^2 \rangle (1 - \xi), \quad (3.8)$$

using the approximation  $\ln(1+x) \approx x$  for  $|x| \ll 1$ . Since  $\xi$  is by definition positive, finite instrumental resolution leads thus to an underestimation of atomic position fluctuations.

## B. Regularization of $L_{\alpha, \tau}(\omega)$

The calculation of the attenuation factor  $\xi$  defined in Eq. (3.5) requires the evaluation of the convolution integral

$$(r * L_{\alpha, \tau})(\omega) = \int_{-\infty}^{+\infty} d\omega' r(\omega - \omega') L_{\alpha, \tau}(\omega')$$

and thus an integration of  $L_{\alpha, \tau}(\omega')$  over the singularity of the latter at  $\omega' = 0$ . For the following calculations we will regularize  $L_{\alpha, \tau}(\cdot)$ , such that such integrations are possible. For this purpose we define

$$\psi_\eta(t) = \psi(t) \exp(-\eta|t|), \quad (3.9)$$

where  $\psi(t)$  is given by Eq. (2.15) and  $\eta > 0$  is a small positive parameter, such that

$$L_{\alpha, \tau}^\eta(\omega) = 2\Re\{\hat{\psi}(i\omega + \eta)\}, \quad (3.10)$$

where  $\hat{\psi}(s)$  is given by Eq. (2.16). Writing

$$\eta + i\omega = \tilde{\omega} \exp(i\phi), \quad \tilde{\omega} = \sqrt{\omega^2 + \eta^2}, \quad (3.11)$$

one obtains

$$L_{\alpha, \tau}^\eta(\omega) = \frac{2\{(\tilde{\omega}\tau)^\alpha \cos \phi + \cos[(\alpha - 1)\phi]\}}{\tilde{\omega}\{(\tilde{\omega}\tau)^\alpha + 2 \cos \alpha\phi + (\tilde{\omega}\tau)^{-\alpha}\}}. \quad (3.12)$$

For  $\eta \rightarrow 0$  we have  $\phi = \pi/2$  and  $L_{\alpha, \tau}(\omega)$  given in Eq. (2.18) is retrieved. In contrast to the latter, the regularized version stays finite at  $\omega = 0$ ,

$$L_{\alpha, \tau}^\eta(0) = \frac{2}{\eta(1 + (\eta\tau)^{-\alpha})}. \quad (3.13)$$

## C. Estimating the position fluctuations for a Gaussian resolution function

Let us suppose that the instrumental resolution of the spectrometer, which is used to measure the neutron scattering intensity, is given by a normalized Gaussian ( $\sigma > 0$ ),

$$r(\omega) = \frac{\exp(-\omega^2/2\sigma^2)}{\sqrt{2\pi}\sigma}, \quad (3.14)$$

with a HWHM of

$$\Gamma \approx 1.17\sigma. \quad (3.15)$$

In order to estimate the attenuation factor  $\xi$  defined in Eq. (3.5), we use the convolution theorem of the Fourier transform and write

$$\begin{aligned} \frac{1}{2\pi} (r * L_{\alpha, \tau})(\omega) &= \lim_{\eta \rightarrow 0^+} \int_{-\infty}^{+\infty} dt \exp(-i\omega t) R(t) \\ &\quad \times E_\alpha(-[|t|/\tau]^\alpha) \exp(-\eta|t|), \end{aligned} \quad (3.16)$$

where

$$R(t) = \frac{\exp(-\frac{1}{2}\sigma^2 t^2)}{2\pi} \quad (3.17)$$

and  $E_\alpha(-[|t|/\tau]^\alpha)$  are, respectively, is the inverse Fourier transform of  $r(\omega)$  and  $L_{\alpha, \tau}(\omega)$ . At this point one can use the decomposition (2.20) for  $\psi(t) = E_\alpha(-[|t|/\tau]^\alpha)$ , where  $p_{\tau, \alpha}(\lambda)$

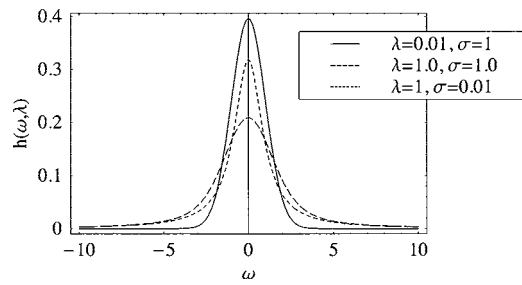


FIG. 2. The function  $h(\omega, \lambda)$  given by expression (3.20) for three combinations of  $\lambda$  and the width parameter  $\sigma$  of the Gaussian resolution function.

is given by expression (2.23). Defining the auxiliary function

$$h(\omega, \lambda) = \int_{-\infty}^{+\infty} dt \exp(-i\omega t) R(t) \exp(-\lambda|t|), \quad (3.18)$$

one obtains thus

$$\frac{1}{2\pi} (r * L_{\alpha, \tau})(\omega) = \int_0^{\infty} d\lambda p_{\alpha, \tau}(\lambda) h(\omega, \lambda). \quad (3.19)$$

The above expression can be computed by numerical integration, taking advantage of the fact that an analytical expression for  $h(\omega, \lambda)$  can be easily obtained. Using the Laplace transform of  $R(t)$ , which has the form<sup>20</sup>  $\hat{r}(s) = \exp(s^2/(2\sigma^2)) \operatorname{erfc}(s/(\sigma\sqrt{2})) / (2\sigma\sqrt{2}\pi)$ , and that the Fourier transform of an even function  $f(t)$  is related to its Laplace transform through  $\bar{f}(\omega) = 2\Re\{\hat{f}(i\omega)\}$ , we obtain from Eq. (3.18)  $h(\omega, \lambda) = 2\Re\{\hat{r}(i\omega + \lambda)\}$ . In explicit form one has<sup>26</sup>

$$h(\omega, \lambda) = \frac{\exp((\lambda^2 - \omega^2)/2\sigma^2)}{\sqrt{2}\pi\sigma} \times \left( \Re \left\{ \operatorname{erfc} \left( \frac{\lambda + i\omega}{\sqrt{2}\sigma} \right) \right\} \cos \left( \frac{\lambda\omega}{\sigma^2} \right) + \Im \left\{ \operatorname{erf} \left( \frac{\lambda + i\omega}{\sqrt{2}\sigma} \right) \right\} \sin \left( \frac{\lambda\omega}{\sigma^2} \right) \right). \quad (3.20)$$

Figure 2 shows the function  $h(\omega, \lambda)$  for three different combinations of  $\lambda$  and the width parameter  $\sigma$  of the resolution function.

$$h(\omega, \lambda) = -\frac{\arg(1 - i\omega_c/(\lambda + i\omega))}{\pi\omega_c} + \frac{\arg(1 + i\omega_c/(\lambda + i\omega))}{\pi\omega_c} + \frac{\omega \arg(1 + \omega_c^2/(\lambda + i\omega)^2)}{\pi\omega_c^2} - \frac{\lambda \log(4\lambda^2\omega_c^4/(\lambda^2 + \omega^2)^4 + (1 + (\lambda^2 - \omega^2)\omega_c^2/(\lambda^2 + \omega^2)^2))}{2\pi\omega_c^2}. \quad (3.28)$$

Figure 3 shows the above function for three different combinations of  $\lambda$  and the cut-off frequency  $\omega_c$ .

### E. The limiting cases $\Gamma \rightarrow 0$ and $\Gamma \rightarrow \infty$

We will now show that the attenuation factor  $\xi$  defined in Eq. (3.5) has the rigorous bounds  $0 \leq \xi \leq 1$ , with  $\xi \rightarrow 0$  for  $\Gamma \rightarrow 0$  and  $\xi \rightarrow 1$  for  $\Gamma \rightarrow \infty$ . For this purpose we introduce the

Since  $p_{\alpha, \tau}(\lambda)$  is singular at  $\lambda=0$ , it is more convenient for the numerical evaluation of expression (3.19) to introduce the new variable

$$u = (\lambda\tau)^\alpha. \quad (3.21)$$

Redefining at the same time

$$\omega \rightarrow \omega\tau, \quad \sigma \rightarrow \sigma\tau, \quad \Gamma \rightarrow \Gamma\tau \quad (3.22)$$

yields

$$\frac{1}{2\pi} (r * L_{\alpha, \tau})(\omega) = \frac{\tau}{\pi\alpha} \int_0^{\infty} du \frac{\sin(\pi\alpha)}{u^2 + 2u \cos(\pi\alpha) + 1} h(\omega, u^{1/\alpha}). \quad (3.23)$$

For  $0 < \alpha < 1$  no singularities are encountered in the integration interval  $(0, \infty)$ . Using expression (3.23), the attenuation factor  $\xi$  may be finally expressed in the dimensionless form

$$\xi = \frac{\int_{-\Gamma}^{+\Gamma} d\omega (1/2\pi) (r * L_{\alpha, 1})(\omega)}{\int_{-\Gamma}^{+\Gamma} d\omega r(\omega)}. \quad (3.24)$$

### D. Estimating the position fluctuations for a triangular resolution function

We assume now that resolution function of the spectrometer is triangular. Instead of Eq. (3.14) we have now ( $\omega_c > 0$ )

$$r(\omega) = \begin{cases} 1/\omega_c(1 - |\omega|/\omega_c) & \text{if } |\omega| \leq \omega_c \\ 0 & \text{otherwise,} \end{cases} \quad (3.25)$$

and the HWHM is given by

$$\Gamma = \omega_c/2. \quad (3.26)$$

To evaluate expression (3.16) we need to compute  $h(\omega, \lambda)$  for a triangular resolution function. Using expression (3.18), the inverse Fourier transform of expression definition (3.25),

$$R(t) = \frac{2 \sin^2(\omega_c t/2)}{\pi\omega_c^2 t^2}, \quad (3.27)$$

and  $h(\omega, \lambda) = 2\Re\{\hat{r}(i\omega + \lambda)\}$ , where  $\hat{r}(s) = 2\omega_c \arctan(\omega_c/s) - s \log(1 + [\omega_c^2/s^2]) / (2\pi\omega_c^2)$ , we find that<sup>26</sup>

dimensionless frequency  $\Omega = \omega/\Gamma$  and the notation  $r(\omega; \Gamma)$  for the resolution function, in order to explicitly indicate the HWHM as a parameter. Since

$$\pi(\omega; \Gamma) = \frac{1}{\Gamma} r\left(\frac{\omega}{\Gamma}; 1\right), \quad (3.29)$$

the attenuation factor  $\xi$  may be cast into the form

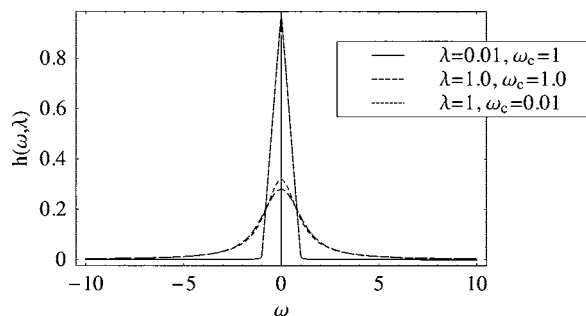


FIG. 3. The function  $h(\omega, \lambda)$  given by expression (3.28) for three combinations of  $\lambda$  and the (angular) cut-off frequency  $\omega_c$  of the triangular resolution function.

$$\xi = \frac{\Gamma \int_{-1}^{+1} d\Omega (1/2\pi) \int_{-\infty}^{+\infty} d\Omega' r(\Omega - \Omega'; 1) L_{\alpha, \tau}^{\eta}(\Gamma\Omega')}{\int_{-1}^{+1} d\Omega r(\Omega; 1)}. \quad (3.30)$$

Here we have used the regularized form  $L_{\alpha, \tau}^{\eta}(\cdot)$ , which stays finite at  $\omega=0$ . In the limit  $\Gamma \rightarrow 0$ , i.e., for an ideal spectrometer, one obtains thus

$$\lim_{\Gamma \rightarrow 0} \xi = 0 \quad \text{for any } \eta > 0. \quad (3.31)$$

In the other extreme case, i.e., for  $\Gamma \rightarrow \infty$ , one may use that

$$\lim_{\Gamma \rightarrow \infty} \frac{\Gamma}{2\omega} L_{\alpha, \tau}^{\eta}(\Gamma\Omega) = \delta(\Omega). \quad (3.32)$$

This relation follows from the scaling property of the Fourier transform  $\lambda \tilde{f}(\lambda\omega) \leftrightarrow f(t/\lambda)$ , with  $f(\cdot)$  being an arbitrary function in the time domain. It follows then that  $\Gamma L_{\alpha, \tau}^{\eta}(\Gamma\Omega) \leftrightarrow \psi_{\eta}(t/\Gamma)$ , where  $t$  is dimensionless, and Eq. (3.32) is obtained in the limit  $\Gamma \rightarrow \infty$ , using that  $\psi_{\eta}(0)=1$ . Inserting identity (3.32) into expression (3.30) one sees easily that

$$\lim_{\Gamma \rightarrow \infty} \xi = 1. \quad (3.33)$$

We find thus  $\xi$  has the rigorous bounds  $0 \leq \xi \leq 1$ , such that

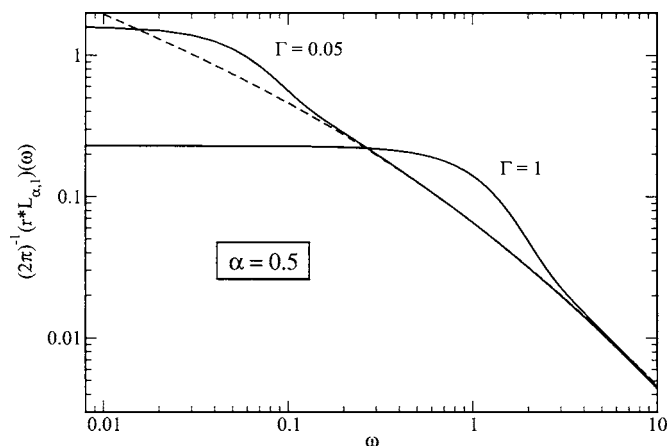


FIG. 4. The function  $(2\pi)^{-1}(r * L_{\alpha,1})(\omega)$  for  $\alpha=0.5$  where  $r(\omega)$  is the Gaussian resolution function defined in Eq. (3.14). Results are shown for  $\Gamma=0.05$  and  $\Gamma=1.0$  (solid lines). The broken line shows the ideal spectrum, where  $\Gamma=0$ .

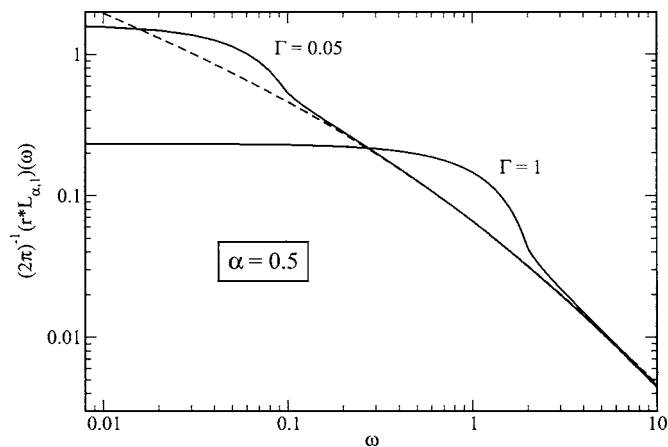


FIG. 5. The same as Fig. 4, but for the triangular resolution function defined in Eq. (3.25).

$$0 \leq \langle x^2 \rangle_m \leq \langle x^2 \rangle. \quad (3.34)$$

## F. Numerical results

The influence of a Gaussian and a triangular resolution function on a hypothetical quasielastic neutron scattering (QENS) spectrum in form of a generalized Lorentzian is shown in Figs. 4 and 5, respectively. In both cases the convolution integral  $(2\pi)^{-1}(r * L_{\alpha,1})(\omega)$  is shown for  $\alpha=0.5$  and a HWHM of  $\Gamma=0.05$  (solid line, upper curve), and for  $\alpha=0.5$  with  $\Gamma=1.0$  (solid line, lower curve). For comparison the scattering intensity for an ideal spectrometer with  $\Gamma=0$  is given (dashed line). All functions are normalized such that the integral over  $\omega$  is one. It should be noted that the convolution regularizes the spectrum at  $\omega=0$ . The reason to choose  $\alpha=0.5$  is motivated by the fact that this value is characteristic for fBD in proteins seen by molecular dynamics simulations and by QENS experiments.<sup>10,11</sup>

Figure 6 shows the attenuation factor  $\xi$  as a function of  $\Gamma\tau$  for two values of  $\alpha$  and for two definitions of elastic scattering, assuming a Gaussian resolution function. The

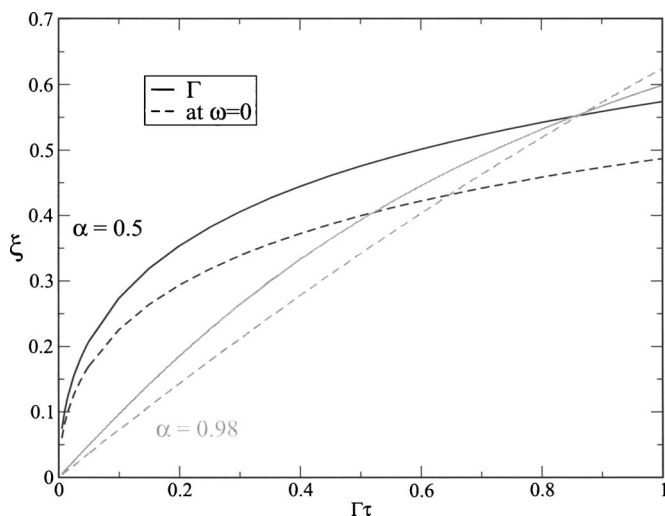


FIG. 6. Attenuation factor  $\xi$  as a function of  $\Gamma\tau$  for  $\alpha=0.5$  (black lines) and  $\alpha=0.98$  (gray lines). The solid lines and dashed lines refer to  $\xi$  as defined in Eqs. (3.5) and (3.6), respectively.

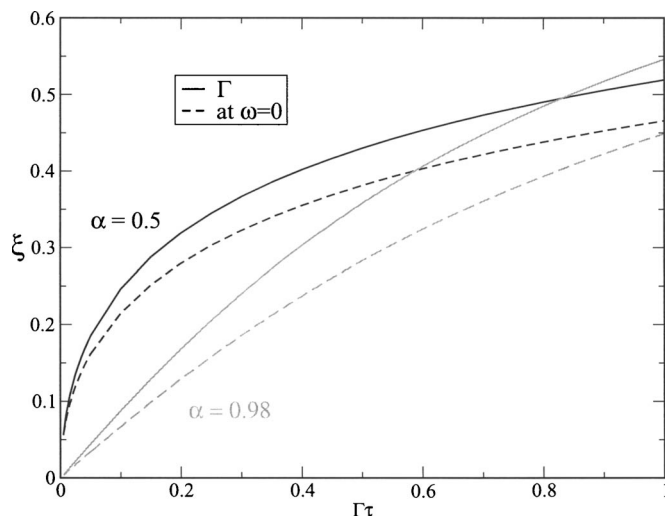


FIG. 7. The same as Fig. 6, but for a triangular resolution function.

black and gray lines correspond, respectively, to  $\alpha=0.5$  and  $\alpha=0.98$ , and the solid and dashed lines refer to  $\xi$  as defined by Eqs. (3.5) and (3.6), respectively. For comparison we show in Fig. 7 the corresponding curves for a triangular resolution function. Defining the elastic scattering intensity by  $S_m(q, 0)$  leads to numerically stable results for the values of  $\Gamma\tau$  used here, which are enclosed in the interval  $0.005 \leq \Gamma\tau \leq 1$ . For small values of  $\Gamma\tau$  the attenuation factor  $\xi$  is considerably larger for  $\alpha=0.5$  than for  $\alpha=0.98$ , which corresponds to a quasielastic scattering spectrum close to a normal Lorentzian. We note that all numerical integrations have been performed with the program MATHEMATICA.<sup>26</sup>

Concrete values for  $\Gamma$  and  $\tau$  can be estimated from the QENS spectrum for a hydrated myoglobin powder at room temperature, which is shown in Fig. 8. The data (squares) have been obtained by Doster *et al.*,<sup>27</sup> combining measurements on the IN6 and IN13 spectrometers at the Institut

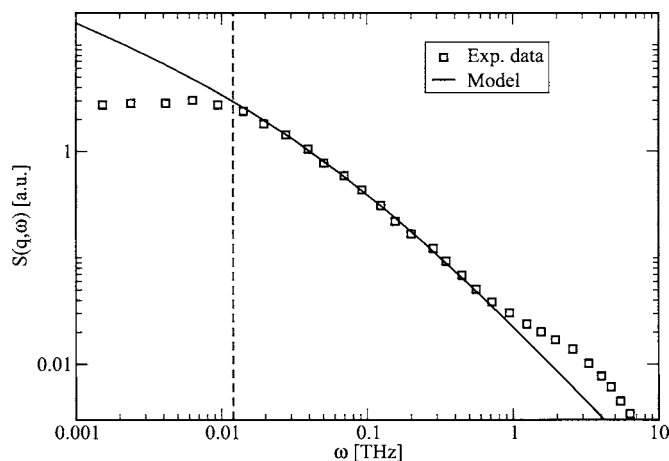


FIG. 8. Fit of model (2.27) to the experimental QENS data in Ref. 1 at 300 K (solid line and squares, respectively). Here  $\omega$  is given on a terahertz (angular) frequency scale. Apart from a global amplitude factor, the fitted parameters are  $\tau=24.12$  ps and  $\alpha=0.51$ . The vertical dashed line indicates the resolution of the spectrometer IN13 at the Institut Laue-Langevin in Grenoble, which is 0.012 THz on the (angular) frequency scale, corresponding to  $8 \mu\text{eV}$  on the energy transfer scale. For use with Fig. 6 one notes that here  $\Gamma\tau=0.29$ .

Laue-Langevin in Grenoble. The latter is a high resolution backscattering spectrometer and has a resolution of  $8 \mu\text{eV}$ , corresponding to  $\Gamma=0.012$  THz (angular frequency). The solid line shows a fit of the model given in Eq. (2.27). Here the first five terms in the series have been used, yielding  $\alpha=0.51$  and  $\tau=24.12$  ps.<sup>10</sup> Similar values for  $\alpha$  and  $\tau$  have been found by analyzing the mean square displacement obtained by molecular dynamics simulations of lysozyme.<sup>10</sup> With  $\tau=24.12$  ps one obtains  $\Gamma\tau=0.29$  and a corresponding attenuation factor  $\xi \approx 0.40$  for a Gaussian resolution function and  $\xi \approx 0.36$  for a triangular resolution function, applying definition (3.5) for the attenuation factor  $\xi$ .

#### IV. CONCLUSION

In this article we have studied the influence of finite instrumental resolution on the elastic incoherent neutron scattering intensities from hydrated protein powders. We estimated, in particular, the resulting corrections for the mean square position fluctuations of the protein hydrogen atoms, which can be extracted from such experiments. The idea was to use fractional Brownian dynamics of a particle in a harmonic potential as a model for the motion of a “representative” hydrogen atom, in order to construct the missing part of the quasielastic neutron scattering profile which is not accessible due to finite instrumental resolution. The model is characterized by a wide spectrum of relaxation rates and has proven to be appropriate to describe protein motion on time scales from subnanoseconds to hours. Our study shows that the corrections of the mean atomic position fluctuations depend strongly on the model parameter  $\alpha$  describing the deviation from normal Lorentzian scattering profiles, which are characterized by  $\alpha=1$  and a single characteristic relaxation rate. Comparing the cases of  $\alpha=0.5$ , which has been found by several experimental and simulation studies of slow protein dynamics, and  $\alpha$  close to one, we find, in particular, that the assumption of a scattering profile close to a normal Lorentzian leads to an underestimation of the correction for the position fluctuations if  $\Gamma\tau \ll 1$ , where  $\tau$  is the time scale parameter of the model and  $\Gamma$  the resolution of the instrument. The results suggest that studies of the dynamical transition seen in most proteins at temperatures of about 200 K must be interpreted with care. Here one considers typically the evolution of the mean square position fluctuation with temperature, and one can assume that the latter has a strong impact on the time scale parameter  $\tau$ , leading thus to considerable variations in the corrections for the observed position fluctuations.

<sup>1</sup> W. Doster, S. Cusack, and W. Petry, *Nature (London)* **337**, 754 (1989).

<sup>2</sup> S. Cusack and W. Doster, *Biophys. J.* **58**, 248 (1990).

<sup>3</sup> W. Doster, S. Cusack, and W. Petry, *Phys. Rev. Lett.* **65**, 1080 (1990).

<sup>4</sup> G. R. Kneller and J. C. Smith, *J. Mol. Biol.* **242**, 181 (1994).

<sup>5</sup> H. Yang, G. Luo, P. Karnchanaphanurach, T. M. Louie, I. Rech, S. Cova, L. Xun, and X. S. Xie, *Science* **302**, 262 (2003).

<sup>6</sup> W. G. Glöckle and T. F. Nonnenmacher, *Biophys. J.* **68**, 46 (1995).

<sup>7</sup> K. B. Oldham and J. Spanier, *The Fractional Calculus* (Academic, New York, 1974).

<sup>8</sup> H. Yang and X. S. Xie, *J. Chem. Phys.* **117**, 10965 (2002).

<sup>9</sup> M. C. Wang and G. E. Uhlenbeck, *Phys. Rev.* **93**, 249 (1945).

<sup>10</sup> G. R. Kneller, *Phys. Chem. Chem. Phys.* **7**, 2641 (2005).

<sup>11</sup> G. R. Kneller and K. Hinsen, *J. Chem. Phys.* **121**, 10278 (2004).

- <sup>12</sup>G. Zaccai, *Science* **288**, 1604 (2000).
- <sup>13</sup>K. Hinsén, A.-J. Petrescu, S. Dellerue, M. C. Bellissent-Funel, and G. R. Kneller, *Condensed Phase Structure and Dynamics: A Combined Neutron Scattering and Molecular Modelling Approach*, special issue of *Chem. Phys.* **261**, 25 (2000).
- <sup>14</sup>F. Volino and A. J. Dianoux, *Mol. Phys.* **41**, 271 (1980).
- <sup>15</sup>F. Gabel, *Eur. Biophys. J.* **34**, 1 (2005).
- <sup>16</sup>T. Becker and J. C. Smith, *Phys. Rev. E* **67**, 021904 (2003).
- <sup>17</sup>R. Metzler and J. Klafter, *Phys. Rep.* **339**, 1 (2000).
- <sup>18</sup>C. W. Gardiner, *Handbook of Stochastic Methods*, Springer Series in Synergetics Vol. 13, 2nd ed. (Springer, Berlin, 1985).
- <sup>19</sup>H. Risken, *The Fokker-Planck Equation*, Springer Series in Synergetics Vol. 18, 2nd reprinted ed. (Springer, Berlin, 1996).
- <sup>20</sup>M. Abramowitz and I. A. Stegun, *Handbook of Mathematical Functions* (Dover, New York, 1972).
- <sup>21</sup>A. Erdélyi, W. Magnus, F. Oberhettinger, and F. G. Tricomi, *Higher Transcendental Functions* (McGraw Hill, New York, 1955).
- <sup>22</sup>J. H. Schwarz, *J. Math. Phys.* **46**, 013501 (2005).
- <sup>23</sup>S. W. Lovesey, *Theory of Neutron Scattering from Condensed Matter* (Clarendon, Oxford, 1984), Vol. I.
- <sup>24</sup>M. Bée, *Quasielastic Neutron Scattering: Principles and Applications in Solid State Chemistry, Biology and Materials Science* (Adam Hilger, Bristol, 1988).
- <sup>25</sup>J. P. Boon and S. Yip, *Molecular Hydrodynamics* (McGraw Hill, New York, 1980). See Eqs. (3.5.23), (3.5.33), and (3.5.37), and the corresponding references.
- <sup>26</sup>MATHEMATICA 5.0, Wolfram Research Inc., 100 Trade Center Drive Champaign, IL 61820-7237.
- <sup>27</sup>W. Doster, S. Cusack, and W. Petry, *Nature (London)* **337**, 754 (1989).